THE JOURNAL OF BIOLOGICAL CHEMISTRY
Vol. 279, No. 22, Issue of May 28, pp. 23806–23812, 2004
Printed in U.S.A.

Regulation of NDR2 Protein Kinase by Multi-site Phosphorylation and the S100B Calcium-binding Protein*

Received for publication, March 4, 2004
Published, JBC Papers in Press, March 22, 2004, DOI 10.1074/jbc.M402472200

Mario R. Stegert‡, Rastislav Tamaskovic§, Samuel J. Bichsel¶, Alexander Hergovich‖, and Brian A. Hemmings**

From the Friedrich Miescher Institute for Biomedical Research, Maulbeerstrasse 66, CH 4058 Basel, Switzerland

Nuclear Dbf2-related (NDR) protein kinases are a family of AGC group kinases that are involved in the regulation of cell division and cell morphology. We describe the cloning and characterization of the human and mouse NDR2, a second mammalian isoform of NDR protein kinase. NDR1 and NDR2 share 86% amino acid identity and are highly conserved between human and mouse. However, they differ in expression pattern; mouse *Ndr1* is expressed mainly in spleen, lung and thymus, whereas mouse *Ndr2* shows highest expression in the gastrointestinal tract. NDR2 is potently activated in cells following treatment with the protein phosphatase 2A inhibitor okadaic acid, which also results in phosphorylation on the activation segment residue Ser-282 and the hydrophobic motif residue Thr-442. We show that Ser-282 becomes autophosphorylated *in vivo*, whereas Thr-442 is targeted by an upstream kinase. This phosphorylation can be mimicked by replacing the hydrophobic motif of NDR2 with a PRK2-derived sequence, resulting in a constitutively active kinase. Similar to NDR1, the autophosphorylation of NDR2 protein kinase was stimulated *in vitro* by S100B, an EF-hand Ca^{2+}-binding protein of the S100 family, suggesting that the two isoforms are regulated by the same mechanisms. Further we show a predominant cytoplasmic localization of ectopically expressed NDR2.

The NDR[1] protein kinase family is a member of the AGC[2] group of serine/threonine kinases, which includes cAMP-dependent kinase, cGMP-dependent kinase, protein kinase B, and protein kinase C (1). The human NDR protein kinase is highly conserved and is expressed almost ubiquitously (2). The closest members of the mammalian NDR protein kinase from lower organisms, TRC, SAX-1, Cbk1p, and Orb6p, are all involved in the control of cell morphology. The *Drosophila* NDR kinase TRC regulates the integrity of epidermal cell extensions such as sensory bristles, arista, and wing hairs by affecting the actin cytoskeleton and is proposed to form a part of a putative morphogenetic checkpoint (3). SAX-1 is the *Caenorhabditis elegans* NDR protein kinase and is reported to play an important role in the regulation of neuronal cell shape and neurite initiation (4). The relatives of NDR protein kinase in *Saccharomyces cerevisiae* and *Schizosaccharomyces pombe*, Cbk1 and Orb6, are also essential for normal morphogenesis, cell polarity, and coordination of cell morphology with the cell cycle (5–8).

NDR protein kinase and its relatives have a conserved structure consisting of an N-terminal S100B/calmodulin binding site, a catalytic kinase domain containing an insertion between subdomains VII and VIII (encompassing, in the case of NDR, a nonconsensus nuclear localization signal and the activation segment phosphorylation site), and a C-terminal regulatory domain (2, 9, 10). The human NDR1 protein has been shown to become autophosphorylated on Ser-281 and activated upon S100B binding in a Ca^{2+}-dependent manner. The C-terminal regulatory phosphorylation site Thr-444 is phosphorylated *in vivo* by a so far unidentified upstream kinase (11). This phosphorylation within the hydrophobic motif, which is an event typical of the regulation of many AGC group kinases, promotes kinase activation and protein stability (12, 13). Some kinases, such as PRK2, have an Asp residue instead of a Ser or Thr residue, and a mutation of the hydrophobic phosphorylation site of to an Asp was shown to result in a constitutively active hydrophobic motif for several kinases (14, 15).

Here we describe the characterization of a second isoform of NDR protein kinase, termed NDR2, and show that m*Ndr1* is widely expressed, whereas m*Ndr2* is expressed mainly in the gastrointestinal tract of mice. NDR2 becomes activated *in vivo* following phosphorylation on three conserved sites, Thr-75, Ser-282, and Thr-442. Further, a NDR2-PIFtide chimera, which contains the PRK2 hydrophobic motif (PIFtide), is constitutively active. *In vitro*, the Ca^{2+}-binding protein S100B stimulates activation of NDR2 and autophosphorylation on Thr-75, Ser-282, and Thr-444.

EXPERIMENTAL PROCEDURES

PCR and Molecular Cloning—BLAST searches of the NCBI data base were performed to identify NDR-related sequences. The *Ndr2* cDNA was assembled by PCR screening using a Marathon-Ready™ human brain cDNA library (Clontech) following standard protocols (16). The mouse *Ndr1* cDNA was cloned from a mouse λZAPII (Stratagene) cDNA library; the mouse *Ndr2* cDNA was cloned using a 3′ mEST (GenBank™ accession number AA277870) and subcloning the 5′ end from a mouse brain cDNA library (Clontech) using PCR. Sequences of all clones were obtained using an ABI PRISM 3700 DNA Analyzer (Applied Biosystems) using custom-synthesized primers and compared

* The Friedrich Miescher Institute is a part of the Novartis Research Foundation. The costs of publication of this article were defrayed in part by the payment of page charges. This article must therefore be hereby marked "*advertisement*" in accordance with 18 U.S.C. Section 1734 solely to indicate this fact.

The nucleotide sequence(s) reported in this paper has been submitted to the GenBank™/EBI Data Bank with accession number(s) AA292399 (mNdr1) and AA292400 (mNdr2).

‡ Supported, in part, by Bundesamt fuer Bildung und Wissenschaft (BBW) Bern Grant 98.0176 and the Krebsliga beider Basel.

§ Supported by Swiss Cancer League Grant KFS-01342-02-2003.

¶ Supported, in part, by BBW Bern Grant 98.0176.

‖ Supported by the Roche Research Foundation.

** To whom correspondence should be addressed. Tel.: 41-61-697-4872; Fax: 41-61-697-3976; E-mail: brian.hemmings@fmi.ch.

[1] The abbreviations used are: NDR, nuclear Dbf2-related; HA, hemagglutinin; MS, mass spectroscopy; PBS, phosphate-buffered saline; GFP, green fluorescent protein; GST, glutathione *S*-transferase; h, human; m, mouse; OA, okadaic acid.

[2] For abbreviations of protein kinase groups and names, see Manning *et al.* (29).

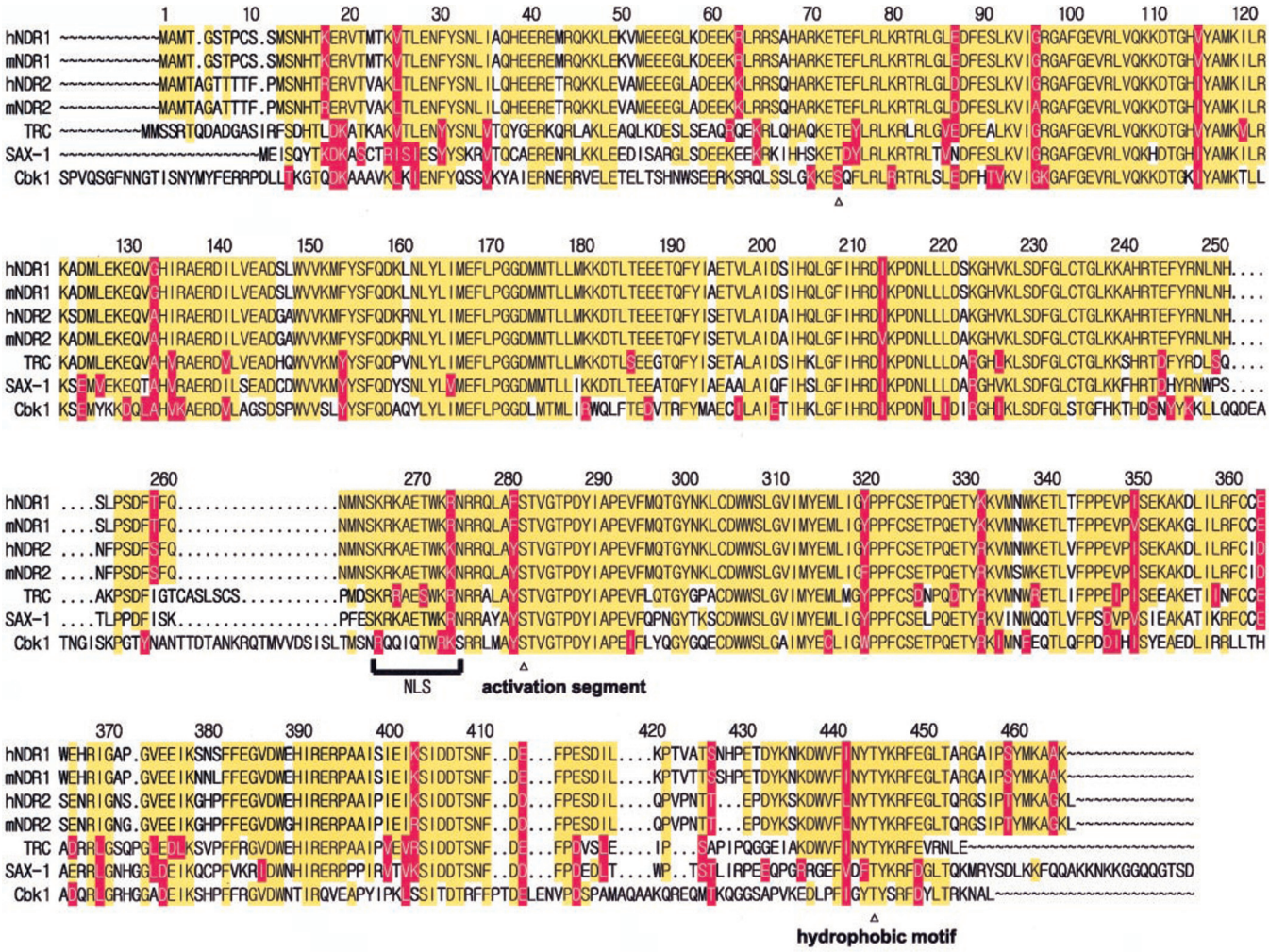

FIG. 1. **Amino acid sequence alignment of *Homo sapiens*, *Mus musculus*, *D. melanogaster*, *C. elegans*, and *S. cerevisiae* NDR**. The NDR amino acid sequences were aligned using Seqweb 1.2. Identical amino acids are *shaded* in *yellow* and similar residues in *red*. *Dots* represent gaps inserted to bring the sequences into alignment. The NDR phosphorylation sites Thr-74, Ser-281, and Thr-444 are indicated with *arrows* and *numbered* according to hNDR1. The predicted nuclear localization signal (*NLS*) is indicated.

with the appropriate genomic databases (Ensembl and Celera). Sequence analysis was performed using Seqweb 1.2 (Genetics Computer Group, Inc.).

Plasmids—Mammalian expression vectors encoding HA and GST epitope-tagged hNDR1 were described previously (2). Expression vectors for HA-hNDR2 and GST-NDR2 were constructed similarly. GFP-Ndr2 was constructed by amplifying the Ndr2 cDNA with primers 5′-CGGGATCCGGTACCATGGCAATGACGG-CAGGGACTAC-3′ and 5′-CGGGATCCCTTCATTCATAACTTCCCAGC-3′ using *Pfu* polymerase (Promega). The PCR product was then digested with BamHI and cloned into pEGFP-C1 (Clontech). HA-NDR2-PIFtide was constructed by amplifying NDR2 cDNA with primers 5′-CTTCCAAGCTTAGTCGA-CATGGCTTACCCATACGATGTTCCAGATTACGCTTCGGCAATGAC-GGCAGGGACTACAACAACC-3′ and 5′-CGGGATCCTCACCAGTCGG-CGATGTAGTCGAAGTCGCGGAACATCTCCTGCTCCTCTTTGTAGT-CCGGTTCTGTGGTTATT-3′ using *Pfu* polymerase (Promega). The PCR product was then digested with BamHI and SalI and cloned into pCMV5. All plasmids were confirmed by sequence analysis.

RNA Extraction and Real-time Reverse Transcription-PCR—Tissues of three 129SvPas mice were isolated and subjected to RNA extraction using TRIzol reagent (Invitrogen) and the RNeasy 96 kit (Qiagen). Reverse transcription reactions were performed using the GeneAmp RNA PCR kit according to the manufacturer's instructions (Applied Biosystems). Real-time quantitative PCR analysis was performed using an ABI Prism 7700 Sequence Detector. Specific primers and probes for each gene were designed using Primer Express 2.0 software. Amplicon sizes were 67 bp for m*Ndr1* and 98 bp for m*Ndr2*. *Taq*Man PCR reactions were performed for m*Ndr1*, m*Ndr2*, and 18 S rRNA according to the user's manual. Details of primers and probes are available on request. Relative quantitations were performed by comparing the corrected C_t value of each tissue to the corrected C_t value of the brain, as described in the ABI PRISM 7700 User Bulletin No. 2.

Bacterial Expression and Kinase Assay of Human GST-fused NDR2—Expression of pGEX-2T_NDR2 species in the BL21-DE3 (pRep4) *Escherichia coli* strain and *in vitro* kinase assays (autophosphorylation in presence or absence of 100 μM $CaCl_2$ and 10 μM bovine S100B (Sigma)) were performed as described previously for NDR1 (11).

Cell Culture and HA-NDR2 Kinase Assay—Culture, transfection of COS-1 and COS-7 cells, and measurement of kinase activity of HA-NDR2 variants were as described previously for HA-NDR1 (9).

Western Blotting—Immunodetection of NDR2 phosphorylated on Thr-75, Ser-282, or Thr-442 was as described previously (11).

Mass Spectrometry—Analysis of the phosphorylation sites of GST-NDR2 was performed according to Tamaskovic *et al.* (11).

Immunofluorescence Microscopy—Exponentially growing cells were plated on coverslips and transfected the next day with indicated constructs using FuGENE 6 (Roche) as described by the manufacturer. After 24 h of transfection, cells were washed with PBS and fixed in 3% paraformaldehyde, 2% sucrose in PBS at pH 7.4 for 10 min at 37 °C. They were then permeabilized using 0.2% Triton X-100 in PBS for 2 min at room temperature. All subsequent steps were carried out at room temperature. Coverslips were rinsed twice with PBS and incubated for 1 h with anti-HA Y11 (Santa Cruz Biotechnology) diluted in PBS containing 1% BSA, 1% goat serum. After three 1-min washes in PBS, goat anti-rabbit fluorescein isothiocyanate (Sigma) was used as secondary antibody. DNA was counterstained with 4 μg/ml Hoechst (Sigma). Coverslips were then inverted into 5 μl of Vectashield medium (Vector Laboratories). Images were obtained with an Eclipse E800 microscope using a CoolPix950 digital camera (Nikon) and processed using Adobe Photoshop 6.0 (Adobe Systems Inc.). Only cells with intact nuclei were

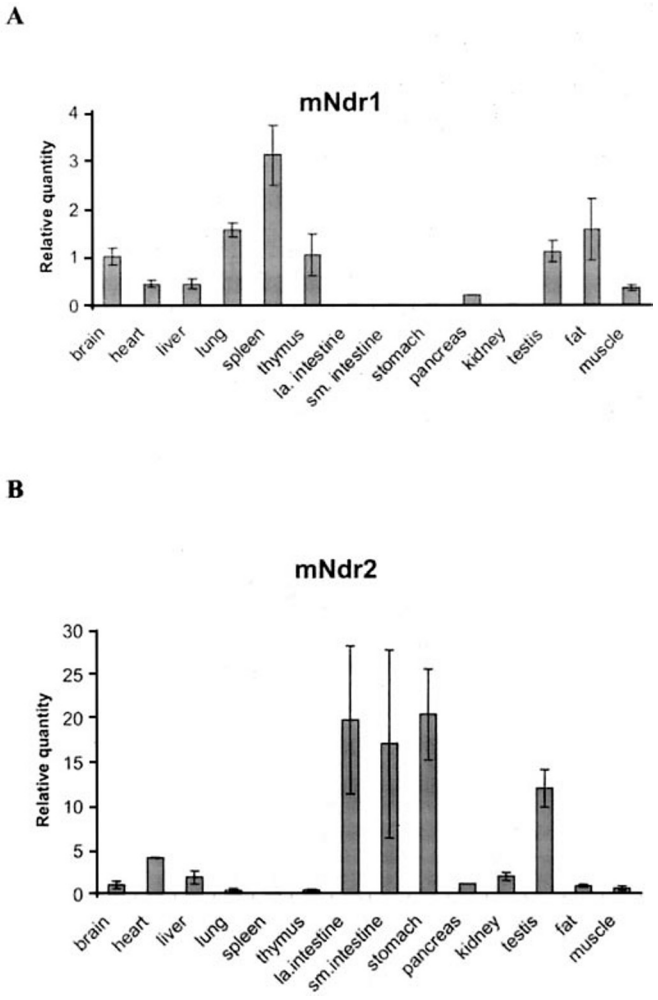

FIG. 2. **Relative mRNA expression levels of m*Ndr1* (*A*) and m*Ndr2* (*B*) determined by quantitative real-time PCR**. The expression levels of m*Ndr1* and m*Ndr2* are shown. RNA samples from three mice were collected and reverse transcribed. Each value was normalized against the expression of 18 S RNA and compared with the relative expression of m*Ndr1* or m*Ndr2* in the brain.

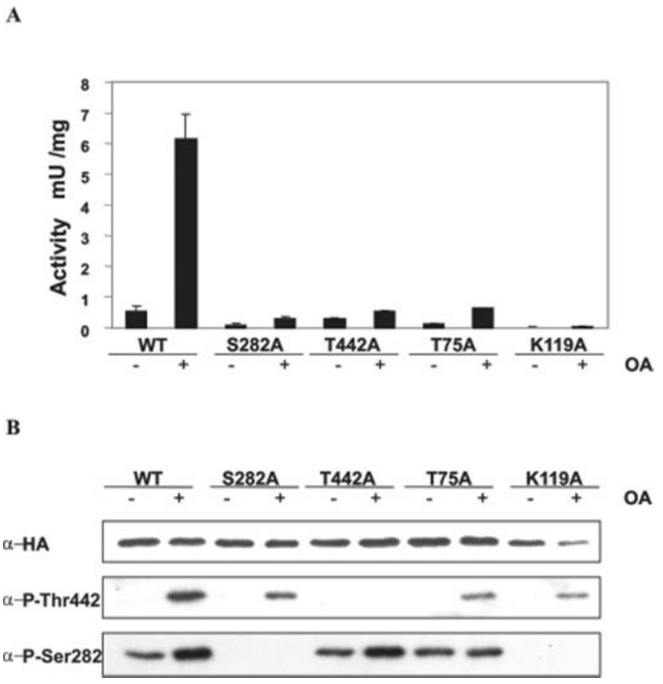

FIG. 3. **NDR2 kinase activity and phosphorylation status of NDR kinase mutants.** *A*, COS-1 cells expressing either wild-type HA-NDR2 (*WT*) or the indicated mutants were treated for 1 h with 1 μM OA or with solvent alone. HA-tagged NDR kinase variants were then immunoprecipitated (100 μg of cell-free protein extracts) with 12CA5 monoclonal antibody and assayed for kinase activity using a peptide substrate as described under "Experimental Procedures." *Bars* represent the mean ± S.D. of triplicate immunoprecipitations. *B*, an aliquot (100 μg of protein) of 12CA5-immunoprecipitated proteins from transfected COS-1 cells was immunoblotted with 12CA5 to verify similar expression levels of each HA-NDR2 construct (*top panel*). For the analysis of phosphorylation status, 12CA5-immunoprecipitated HA-NDR2 variants (100 μg of protein) were analyzed by immunoblotting with phosphospecific antibodies directed against phosphorylated Ser-282 or phosphorylated Thr-442 (*middle* and *bottom panel*, respectively).

included in the statistical evaluation. Cells expressing GFP-NDR2 were fixed and then stained for DNA without permeabilization and antibody incubation steps.

RESULTS

Conservation of NDR Kinases—BLAST searches of the NCBI data base identified the human KIAA0965 clone (GenBank™ accession number AB023182/hj06174s1) as a partial cDNA with significant homology to human NDR1 protein kinase. We determined the sequences of h*Ndr2*, m*Ndr1*, and m*Ndr2* cDNAs and the corresponding mouse genes. The deduced amino acids sequences were compared and aligned to the known sequences of hNDR1, *Drosophila melanogaster* NDR TRC, *C. elegans* NDR SAX-1, and *S. cerevisiae* Cbk1 (Fig. 1*A*). The human and mouse NDR1 sequences show 99% identity, the NDR2 sequences show 97% identity, and NDR1 and NDR2 show an identity of 86%, indicating an extremely high sequence conservation during evolution ranging to flies (68%), worms (67% identity), and yeast (47% identity). Human and mouse NDR2 are 464 amino acids long with a predicted mass of 54 kDa. Gene mapping indicates that h*Ndr1* and m*Ndr1* as well as h*Ndr2* and m*Ndr2* are located on orthologous regions; h*Ndr1* maps to 6p21 (17) and h*Ndr2* to 12p12.3. The corresponding mouse genes map to 17B1 and 6G2-G3. In addition, pseudogenes of *Ndr2* were found on chromosomes 1D and 8A1.2 of the mouse genome. The human and mouse genes consist of 14 exons with conserved intron-exon boundaries. Exon 1 is a noncoding exon containing 5′-untranslated region, exon 2 contains the start codon, and the stop codon is located in exon 14 (data not shown).

*Tissue-specific Expression of Ndr1 and -2—Taq*Man real-time PCR analysis was used to examine the differential expression of m*Ndr1* and m*Ndr2* in mouse tissues obtained from three different mice (Fig. 2). The expression of 18 S rRNA was used as a reference gene to correct for reverse transcription-PCR efficiency of each sample. The highest expression levels of m*Ndr1* were observed in spleen, lung, thymus, brain, and fat tissue, whereas m*Ndr2* expression was found mainly in the large and small intestine, as well as in the stomach and testis. Assuming similar PCR efficiency for both reactions, m*Ndr2* appears to be the predominantly expressed isoform in mice. These data suggest tissue-specific functions of NDR1 and NDR2 in mammals.

Regulation of NDR2 Kinase Activity—A comparison of the NDR2 and NDR1 sequences showed that NDR2 contains three conserved phosphorylation sites corresponding to the described NDR1 phosphorylation sites Thr-75, Ser-281, and Thr-444 (10). NDR2 mutants were created in which Thr-75, Ser-282, or Thr-442 was replaced by an alanine, and a kinase-dead mutant, K119A, was also made. The protein kinase activity of each of these mutants was measured following treatment of transfected COS-1 cells with 1 μM okadaic acid (OA) or with solvent alone for 1 h. HA-NDR2-WT was potently stimulated (~10-fold) by OA (Fig. 3). All three phosphorylation site mutants

(T75A, S282A, and T442A) displayed reduced basal activity and could not be stimulated by treatment with OA. The K119A mutation reduced basal activity to almost undetectable levels and, as expected, abolished the activation by OA. Western blot analysis of the regulatory phosphorylation site mutants T75A, S282A, T442A, and wild type with phospho-specific antibodies, which recognize the phospho-epitopes Ser-282P and Thr-442P, showed that NDR2 became phosphorylated on Ser-282 in wild type, T442A, and T75A and that this phosphorylation increased after OA treatment with the wild type and T442A but not with the mutant T75A. The kinase-dead K119A mutant was not phosphorylated on Ser-282, indicating that Ser-282 is an autophosphorylation site. Thr-442 became phosphorylated upon OA treatment in NDR2 wild type, as well as in the S282A, T75A, and K119A mutants, suggesting that Thr-442 is phosphorylated independently of NDR2 activity and is therefore targeted by an upstream kinase (Fig. 3). These results confirmed that phosphorylation on both the activation segment phosphorylation site Ser-282 and the regulatory hydrophobic motif phosphorylation site Thr-442 is required for NDR2 activation. In addition, NDR2 activity also depends on the presence of Thr-75 in the N-terminal regulatory domain.

Constitutively Active NDR2—The phosphorylation of Ser/Thr residues can be mimicked by substitution of Asp or Glu for several kinases (14). However, we have recently shown that T444D or T444E mutations have only a very moderate effect (1.5–2-fold activation) on NDR1 kinase activity (10). Previous studies with protein kinase B showed that activation of the kinase and engagement of the N-terminal lobe hydrophobic groove, which is dependent on an ordered α-C helix, could also be achieved by substituting the hydrophobic motif of protein kinase B with the constitutive active hydrophobic motif of PRK2 (PIFtide) (15). Based on the similarities of AGC group kinases, we created an NDR2-PIFtide chimera, aiming to generate an active kinase. Indeed, the NDR2-PIFtide had a more than 20-fold elevated basal kinase activity and even showed an increase in activity compared with OA-stimulated NDR2 (Fig. 4*A*). Phosphorylation site analysis showed increased Ser-282 phosphorylation in the NDR2-PIFtide chimera, suggesting an increased autophosphorylation activity (Fig. 4*B*). Therefore, we have shown that substitution of the hydrophobic motif of NDR2 with the PIFtide sequence results in a constitutively active NDR2 kinase, thus describing for the first time a constitutively active variant of the NDR protein kinase.

Activation of NDR2 by S100B—The sequence conservation between NDR1 and NDR2 also encompasses the previously defined S100B-binding domain of NDR1 (see Fig. 1). Therefore, the *in vitro* effect of Ca^{2+}/S100B on NDR2 activity was investigated. Ca^{2+}/S100B increased the rate of NDR2 autophosphorylation ~2-fold after a 4-h incubation (Fig. 5*A*) and stimulated specific NDR activity in a concentration-dependent manner ~4-fold (Fig. 5*B*). This suggests that NDR2 activation by Ca^{2+}/S100B also occurs by the mechanism reported for NDR1 (9, 11). After *in vitro* incubation of GST-NDR2 in the presence and absence of Ca^{2+}/S100B, the proteins were digested with trypsin and the resultant mixture analyzed by electrospray ionization-tandem mass spectrometry in a −79 precursor scan (18). This technique measures the mass to charge ratio (*m/z*) of all peptide species liberating a single phosphate group after fragmentation. Five (NDR2-derived) phospho-peptides were identified in both samples (the GST-NDR2 and the GST-NDR2/Ca^{2+}/S100B), corresponding to the phosphorylation sites Thr-75, Ser-282, and Thr-442 (Fig. 5*C*). These results demonstrate that S100B proteins regulate NDR2 by a mechanism similar to that reported for NDR1 (11).

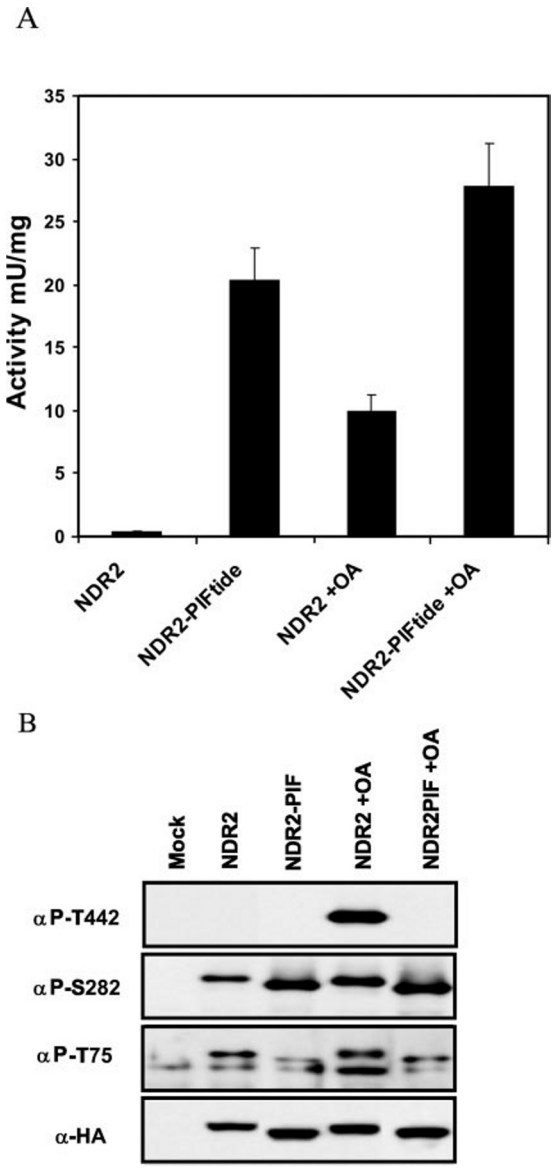

FIG. 4. **NDR2-PIFtide chimera is constitutively active.** *A*, COS-1 cells expressing either wild-type HA-NDR2 or the HA-NDR2-PIFtide chimera were treated for 1 h with 1 μM OA or with solvent alone. HA-tagged NDR kinase variants were then immunoprecipitated (100 μg of cell-free protein extracts) with 12CA5 monoclonal antibody and assayed for kinase activity using a peptide substrate as described under "Experimental Procedures." *Bars* represent the mean ± S.D. of triplicate immunoprecipitations. *B*, for analysis of phosphorylation status, 12CA5-immunoprecipitated HA-NDR2 variants (100 μg of protein) were analyzed by immunoblotting with phosphospecific antibodies directed against phosphorylated Thr-442, phosphorylated Ser-282, or phosphorylated Thr-75 (*top three panels*, respectively). An aliquot (100 μg of protein) of 12CA5-immunoprecipitated proteins from transfected COS-1 cells was immunoblotted with 12CA5 to verify similar expression levels of each HA-NDR2 construct (*bottom panel*).

Localization of NDR2—To examine the subcellular localization of NDR2, COS-7 and HeLa cells were transfected with either N-terminally GFP-tagged NDR2 (GFP-NDR2) or HA-NDR2 and processed for indirect immunofluorescence (Fig. 6*A*; data not shown). A statistical analysis showed that both proteins were detected mainly in the cytoplasm of both COS-7 cells and HeLa cells under these experimental settings (Fig. 6*B*). Similar results were also obtained when U2-OS cells were studied (data not shown). Thus, in marked contrast to the localization pattern described for NDR1 (2), NDR2 was not localized predominantly to nuclear structures. For unknown

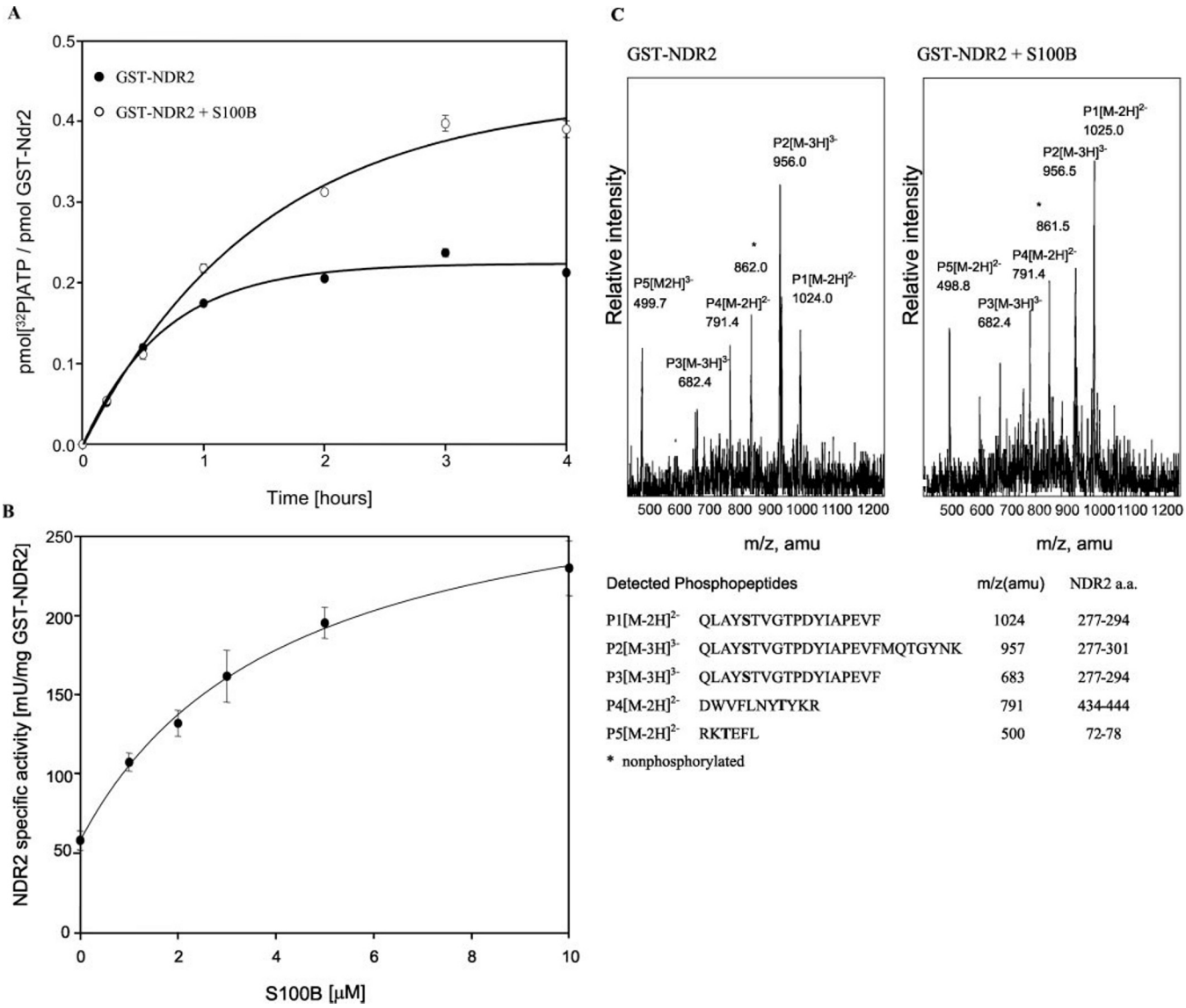

FIG. 5. **Ca^{2+}/S100B promotes the auto- and transphosphorylation of GST-NDR2.** *A*, an aliquot (1 μg) of purified GST-NDR2 wild type (~0.5 μM) was autophosphorylated for the indicated time periods *in vitro* without further additions (*filled circle*) or in the presence of 100 μM $CaCl_2$ and 10 μM bovine S100B (*open circle*) as indicated. *B*, an aliquot (1 μg) of purified GST-NDR2 was autophosphorylated at 30 °C for 2 h in the absence or presence of increasing concentrations of S100B. *C*, mapping of NDR2 *in vitro* autophosphorylation sites. An aliquot (10 μg) of GST-NDR2 was autophosphorylated for 2 h in the absence or presence of 100 μM $CaCl_2$ and 10 μM bovine S100B. After separation by SDS-PAGE, GST-NDR2 was excised and processed by tryptic cleavage for MS analysis of phosphopeptides by precursor ion scanning of *m/z* −79. Phosphopeptides for which *m/z* could be assigned to NDR2-derived phosphopeptides are labeled P1–P5. Some peptides were detected in several charged states, *e.g.* $[M - 2H]^{2-}$, $[M - 3H]^{3-}$. Peptide P1/P3 presumably results from a trace of chymotryptic contamination of the trypsin preparation, because it overlaps with P2 and terminates with an aromatic residue. *Asterisks* denote an abundant, double charged, nonphosphorylated NDR2 peptide (residues 379–392) with *m/z* 862.

reasons, NDR2 was found to be mainly cytoplasmic even though it contains the same NLS as NDR1 (see Fig. 1).

DISCUSSION

In this study, we have described the cloning and characterization of the NDR2 protein kinase, a second isoform of mammalian NDR protein kinase. The extremely high level of conservation of NDR protein kinases throughout the eukaryotic world indicates that this kinase is subject to a very high evolutionary pressure. Mouse and human NDR kinases also show an absolutely conserved gene organization of 14 exons. It is likely that the kinases are components of a conserved signaling pathway (1). This has been shown genetically already for one component of the pathway, the Furry/Mor2/Pag1 protein, mutation of which results in similar phenotypes in *D. melanogaster*, *S. pombe*, and *S. cerevisiae* as reported for NDR kinase mutations (19–21). There is no information on the function of the human Furry protein.

Our results show that NDR2 is regulated by multi-site phosphorylation similar to many of the AGC family of protein kinases. Mutation of one or both phosphorylation site residues, Ser-282 and Thr-442, of NDR2 led to an almost total loss of kinase activity, suggesting that both residues are essential for kinase activity. This is not surprising as similar observations have been made for other AGC group kinases. Recent structural studies of protein kinase B have delineated a mechanism by which multi-site phosphorylation brings about structural changes involving both disorder-to-order transitions of the alpha B and C helices and the ordering of the activation segment, concomitant with converting the kinase to a fully 1000-fold activated enzyme (13, 15). Significantly, NDR2 becomes phos-

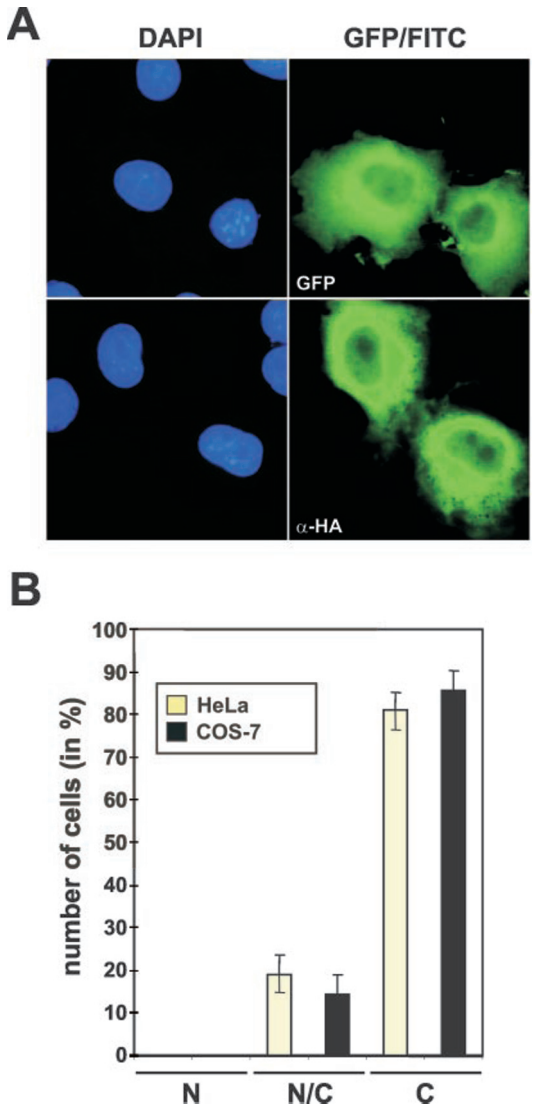

FIG. 6. **NDR2 localizes mainly to cytoplasmic structures.** *A*, COS-7 cells expressing GFP-NDR2 (*upper panels*) or HA-NDR2 (*lower panels*) were processed for immunofluorescence using either no antibody (*upper right*) or anti-HA Y11 (*lower right*). Anti-HA antibody was visualized using anti-rabbit fluorescein isothiocyanate (*FITC*) (*green*). Corresponding DNA stains (*blue; left panels*) are shown. *DAPI*, 4′,6-diamidino-2-phenylindole. *B*, HeLa (*light*) and COS-7 (*dark*) cells expressing GFP-NDR2 were processed for immunofluorescence, and GFP signals were scored as either predominantly nuclear (*N*), nuclear and cytoplasmic (*N/C*), or predominantly cytoplasmic (*C*). The blotted numbers represent at least two independent experiments (±S.D.). A minimum of 150 cells was counted per experiment.

phorylated on three residues *in vitro*. The major site, Ser-282, which is conserved among all AGC group kinases, is an essential part of the activation segment of the kinase. The second site, Thr-75, is located within the S100B-binding domain, and the third site, Thr-442, which is also conserved in the AGC group superfamily, is located outside of the kinase domain in a region enriched with hydrophobic amino acid residues ("hydrophobic motif"). *In vivo* mutation of the phosphorylation site residues Ser-282 and Thr-442 of NDR2 ablated kinase activity and blocked activation. In wild-type NDR2, both residues were phosphorylated upon OA stimulation, whereas in the kinase-dead mutant K119A, only the hydrophobic motif phosphorylation site, Thr-442, was phosphorylated, suggesting that the kinase activity of NDR2 is required only for phosphorylation of Ser-282. Therefore, NDR2 is phosphorylated by an upstream kinase at the C-terminal hydrophobic site in OA-stimulated COS-1 cells. However, we cannot rule out the possibility that Thr-442 autophosphorylation observed *in vitro* also contributes to the overall phosphorylation at this residue *in vivo*. Autophosphorylation on the activation segment residue has also been reported for other members of the AGC kinases such as cAMP-dependent protein kinase and protein kinase Cδ (22, 23). This suggests that autophosphorylation is an alternative mechanism of activation of the few AGC kinases that are not targeted by PDK1 (for review, see Ref. 24). The specificity of activation of AGC group kinases is likely to be mediated by the phosphorylation of the hydrophobic motif residue. For the NDR kinases, some significant clues suggest that upstream kinases are members of the Ste20 family. For example, the upstream kinase of Dbf2 was identified as Cdc15, one of the budding yeast Ste20-like kinases (25), and the fission yeast Ste20-like kinase Pak1/Shk1 was reported to interact genetically with Orb6 (8). The identification of this so far unknown upstream kinase for NDR will provide important information about the physiological regulation of the NDR protein kinase, which in turn could provide hints about the conditions under which this tightly controlled kinase is activated *in vivo*.

As demonstrated for protein kinase B, the PIFtide sequence leads to an ordered structure and therefore fully active hydrophobic motif, concomitant with an activation of the kinase (15). The similarities within the AGC group kinases in sequence similarity and mode of activation enabled us to create a constitutive active NDR2 by substituting the C terminus of NDR2 with the PIFtide sequence. The NDR2-PIFtide showed an even higher activity than the OA-stimulated kinase. This is probably because of an intrinsic stimulation of the autophosphorylation activity by keeping the kinase in the active state, which is also reflected by the increased Ser-282 phosphorylation in the NDR2-PIFtide. The constitutive active kinase will likely prove a valuable tool for the identification of downstream targets of NDR2 protein kinase.

The *in vivo* significance of the phosphorylation at Thr-74 in NDR1 and Thr-75 in NDR2 is unclear thus far. This threonine is within the identified S100B-binding domain of NDR protein kinase, and its mutation is critical for NDR protein kinase activity. This might be because of a missing phosphorylation event or because this residue may be structurally important for the NDR-S100B interaction. Nevertheless, recent data show that Thr-75 is not directly involved in the binding of S100B, suggesting that the phosphorylation modulates the affinity between the two proteins (26). Conservation of the kinase also encompasses the S100B-binding domain, and the mechanism of *in vitro* activation by S100B appears to be identical for NDR1 and NDR2. The homology between the mammalian, fly, worm, and yeast NDR kinases suggests that this mode of activation will be similar in all organisms.

The subcellular localization of NDR2 was rather surprising considering the high sequence similarity between NDR1 and NDR2. Whereas NDR1 was reported to be mainly nuclear (2), we detected NDR2 predominantly localized to cytoplasmic structures in our experimental settings. This might reflect different functions and/or substrate specificities of NDR1 and NDR2 within subcellular compartments.

Most importantly, the two mammalian isoforms differ mainly in their tissue- and cell type-specific expression patterns. It is striking that m*Ndr2* is expressed mainly in highly proliferative tissues with high cellular turnover, such as the stomach and the large and small intestines. Interestingly, h*Ndr1* was recently found to be up-regulated in highly necrotic and progressive ductal carcinoma *in situ*, as well as in some melanoma cell lines (9, 27). Significantly h*Ndr2* is up-regulated in the highly metastatic non-small cell lung cancer cell line

NCI-H460 (28), suggesting a potential role of NDR protein kinase in the regulation of cancer cell morphology and migration.

The major outstanding task for the future will be the full delineation of the novel highly conserved NDR signaling pathway. Of considerable importance is the question of the identification of the predicted agonist and receptor that initiate kinase activation. The answer may then help us understand how NDR contributes to the regulation of cell morphogenesis and proliferation and how these signals are disrupted in transformed cells. Mouse knockout studies may reveal whether the observed differences in tissue-specific expression and subcellular localization of NDR1 and NDR2 reflect differences in their functions.

Acknowledgments—We thank Daniel Hess, Hélène Rogniaux, and Jan Hofsteenge for technical support during the MS analysis.

REFERENCES

1. Tamaskovic, R., Bichsel, S. J., and Hemmings, B. A. (2003) *FEBS Lett.* **546,** 73–80
2. Millward, T., Cron, P., and Hemmings, B. A. (1995) *Proc. Natl. Acad. Sci. U. S. A.* **92,** 5022–5026
3. Geng, W., He, B., Wang, M., and Adler, P. N. (2000) *Genetics* **156,** 1817–1828
4. Zallen, J. A., Peckol, E. L., Tobin, D. M., and Bargmann, C. I. (2000) *Mol. Biol. Cell* **11,** 3177–3190
5. Colman-Lerner, A., Chin, T. E., and Brent, R. (2001) *Cell* **107,** 739–750
6. Bidlingmaier, S., Weiss, E. L., Seidel, C., Drubin, D. G., and Snyder, M. (2001) *Mol. Cell. Biol.* **21,** 2449–2462
7. Racki, W. J., Becam, A. M., Nasr, F., and Herbert, C. J. (2000) *EMBO J.* **19,** 4524–4532
8. Verde, F., Wiley, D. J., and Nurse, P. (1998) *Proc. Natl. Acad. Sci. U. S. A.* **95,** 7526–7531
9. Millward, T. A., Heizmann, C. W., Schafer, B. W., and Hemmings, B. A. (1998) *EMBO J.* **17,** 5913–5922
10. Millward, T. A., Hess, D., and Hemmings, B. A. (1999) *J. Biol. Chem.* **274,** 33847–33850
11. Tamaskovic, R., Bichsel, S. J., Rogniaux, H., Stegert, M. R., and Hemmings, B. A. (2002) *J. Biol. Chem.* **278,** 6710–6718
12. Lang, F., and Cohen, P. (2001) *Science's STKE* **108,** RE17
13. Yang, J., Cron, P., Thompson, V., Good, V. M., Hess, D., Hemmings, B. A., and Barford, D. (2002) *Mol. Cell* **9,** 1227–1240
14. Alessi, D. R., Andjelkovic, M., Caudwell, B., Cron, P., Morrice, N., Cohen, P., and Hemmings, B. A. (1996) *EMBO* **15,** 6541–6551
15. Yang, J., Cron, P., Good, V. M., Thompson, V., Hemmings, B. A., and Barford, D. (2002) *Nat. Struct. Biol.* **9,** 940–944
16. Sambrook, J., Fritsch, E. F., and Maniatis, T. (1989) *Molecular Cloning: A Laboratory Manual*, pp. 810–896, Cold Spring Harbor Laboratory Press, Plainview, NY
17. Tripodis, N., Palmer, S., Phillips, S., Milne, S., Beck, S., and Ragoussis, J. (2000) *Genome Res.* **10,** 454–472
18. Carr, S. A., Huddleston, M. J., and Annan, R. S. (1996) *Anal. Biochem.* **239,** 180–192
19. Cong, J., Geng, W., He, B., Liu, J., Charlton, J., and Adler, P. N. (2001) *Development* **128,** 2793–2802
20. Du, L. L., and Novick, P. (2002) *Mol. Biol. Cell* **13,** 503–514
21. Hirata, D., Kishimoto, N., Suda, M., Sogabe, Y., Nakagawa, S., Yoshida, Y., Sakai, K., Mizunuma, M., Miyakawa, T., Ishiguro, J., and Toda, T. (2002) *EMBO J.* **21,** 4863–4874
22. Yonemoto, W., McGlone, M. L., Grant, B., and Taylor, S. S. (1997) *Protein Eng.* **10,** 915–925
23. Le Good, J. A., Ziegler, W. H., Parekh, D. B., Alessi, D. R., Cohen, P., and Parker, P. J. (1998) *Science* **281,** 2042–2045
24. Leslie, N. R., Biondi, R. M., and Alessi, D. R. (2001) *Chem Rev.* **101,** 2365–2380
25. Mah, A. S., Jang, J., and Deshaies, R. J. (2001) *Proc. Natl. Acad. Sci.* **98,** 7325–7330
26. Bhattacharya, S., Large, E., Heizmann, C. W., Hemmings, B., and Chazin, W. J. (2003) *Biochemistry* **42,** 14416–14426
27. Adeyinka, A., Emberley, E., Niu, Y., Snell, L., Murphy, L. C., Sowter, H., Wykoff, C. C., Harris, A. L., and Watson, P. H. (2002) *Clin. Cancer Res.* **8,** 3788–3795
28. Ross, D. T., Scherf, U., Eisen, M. B., Perou, C. M., Rees, C., Spellman, P., Iyer, V., Jeffrey, S. S., Van de Rijn, M., Waltham, M., Pergamenschikov, A., Lee, J. C., Lashkari, D., Shalon, D., Myers, T. G., Weinstein, J. N., Botstein, D., and Brown, P. O. (2000) *Nat. Genet.* **24,** 227–235
29. Manning, G., Whyte, D. B., Martinez, R., Hunter, T., and Sudarsanam, S. (2002) *Science* **298,** 1912–1934